

This is a repository copy of *Seeing distinct groups where there are none : spurious patterns from between-group PCA*.

White Rose Research Online URL for this paper:

<https://eprints.whiterose.ac.uk/152134/>

Version: Accepted Version

Article:

Cardini, A., O'Higgins, Paul orcid.org/0000-0002-9797-0809 and Rohlf, F. J. (2019) Seeing distinct groups where there are none : spurious patterns from between-group PCA. *Evolutionary Biology*. ISSN 1934-2845

<https://doi.org/10.1007/s11692-019-09487-5>

Reuse

Items deposited in White Rose Research Online are protected by copyright, with all rights reserved unless indicated otherwise. They may be downloaded and/or printed for private study, or other acts as permitted by national copyright laws. The publisher or other rights holders may allow further reproduction and re-use of the full text version. This is indicated by the licence information on the White Rose Research Online record for the item.

Takedown

If you consider content in White Rose Research Online to be in breach of UK law, please notify us by emailing eprints@whiterose.ac.uk including the URL of the record and the reason for the withdrawal request.

1 **Seeing distinct groups where there are none: spurious patterns from between-**
2 **group PCA**

3

4 Cardini, Andrea^{1,2}, O'Higgins, Paul^{4,2}, Rohlf, F. James³

5

6

7 **AUTHORS AFFILIATIONS**

8 ¹Dipartimento di Scienze Chimiche e Geologiche, Università di Modena e Reggio Emilia, Via Campi,
9 103 - 41125 Modena – Italy, <https://orcid.org/0000-0003-2910-632X>

10 ²Centre for Forensic Anthropology, The University of Western Australia, 35 Stirling Highway,
11 Crawley WA 6009, Australia

12 ³Department of Anthropology and Department of Ecology and Evolution, Stony Brook University,
13 Stonybrook, NY 11794-4364, <https://orcid.org/0000-0003-0522-3679>

14 ⁴Department of Archaeology and Hull York Medical School, University of York, Heslington, York,
15 YO10 5DD, <https://orcid.org/0000-0002-9797-0809>

16

17 Corresponding Author: F. James Rohlf, e-mail address: f.james.rohlf@stonybrook.edu; tel. 001 631-
18 632-8580

19

20 **KEYWORDS**

21 Covariance, geometric morphometrics, group separation, isotropic model, spurious clustering

22

23 **RUNNING TITLE**

24 Spurious clustering in bgPCA

1 **Abstract**

2

3 Using sampling experiments, we found that, when there are fewer groups than variables, between-groups PCA
4 (bgPCA) may suggest surprisingly distinct differences among groups for data in which none exist. While
5 apparently not noticed before, the reasons for this problem are easy to understand. A bgPCA captures the $g-1$
6 dimensions of variation among the g group means, but only a fraction of the $\sum n_i - g$ dimensions of within-
7 group variation (n_i are the sample sizes), when the number of variables, p , is greater than $g-1$. This introduces a
8 distortion in the appearance of the bgPCA plots because the within-group variation will be underrepresented,
9 unless the variables are sufficiently correlated so that the total variation can be accounted for with just $g-1$
10 dimensions. The effect is most obvious when sample sizes are small relative to the number of variables, because
11 smaller samples spread out less, but the distortion is present even for large samples. Strong covariance among
12 variables largely reduces the magnitude of the problem, because it effectively reduces the dimensionality of the
13 data and thus enables a larger proportion of the within-group variation to be accounted for within the $g-1$ -
14 dimensional space of a bgPCA. The distortion will still be relevant though its strength will vary from case to
15 case depending on the structure of the data (p , g , covariances etc.). These are important problems for a method
16 mainly designed for the analysis of variation among groups when there are very large numbers of variables and
17 relatively small samples. In such cases, users are likely to conclude that the groups they are comparing are much
18 more distinct than they really are. Having many variables but just small sample sizes is a common problem in
19 fields ranging from morphometrics (as in our examples) to molecular analyses.

20

1
2
3
4
5
6
7
8
9
10
11
12
13
14
15
16
17
18
19
20
21
22
23
24
25
26
27
28
29
30
31
32
33
34
35
36

Introduction

As a general trend, modern science tends to generate a very large number of variables (p) from samples that can vary widely in size (n) and often includes few individuals relative to the number of variables. Indeed, the ‘Omics’ revolution, brought forward by the rapid advancement of informatics and molecular biology, offers some of the best examples of this trend. For instance, microarray analyses may include hundreds of genetic markers from a relatively small number of individuals (Culhane et al. 2002 is an example). However, statistically analyzing such high dimensional data with relatively small sample sizes (p/n ratios) is an important and challenging problem.

A variety of methods for dimensionality reduction are available in the statistical literature (Izenman 2008). Among these, principal component analysis (PCA) is still probably the most popular in biology. A PCA is a rigid rotation of the multidimensional space of all the variables followed by a projection of the data onto relatively few orthogonal axes that together account for as much of the overall variance as possible, though there is no reason for the axes themselves to be especially meaningful biologically. When $p \geq n$, a PCA can only extract at most $n-1$ uncorrelated dimensions that, together, contain all the information about the variances and covariances of the original p variables (all p dimensions can be extracted when $p < n$). Often, there are dominant directions of variance so that a relatively small number of PCs may account for most of the variation. The first (higher order) PCs capture the major aspects of covariation in the sample and the later PCs the smaller ones. Bookstein (2017) first brought attention to the Marchenko-Pastur theorem that shows that large p/n ratios cause an exaggeration of the sizes of the eigenvalues for the first PCs relative to those of the last PCs, thus giving a misleading impression of the relative importance of the patterns that they seem to suggest. The initial motivation for the present paper was to investigate whether large p/n ratios might cause problems for the relatively new and increasingly popular type of PCA, between-group PCA (bgPCA). In this method a PCA is performed on the covariance matrix based on the g sample means (rather than on the original data matrix) followed by the projection of the original n samples onto these bgPC axes. Plots of these axes are then used to illustrate the distances between sample means and allow a user to judge the distinctiveness of the groups.

Phenotypic variation is complex and, although the number and choice of morphometric descriptors should be determined by the specific study hypothesis (Oxnard and O’Higgins, 2011), morphometric studies are often exploratory, tending to employ large numbers of variables, which make this discipline typically highly multivariate (Blackith and Reyment 1971). This is intrinsically true for landmark coordinate-based GM (geometric morphometrics), because each additional landmark or semilandmark adds two variables to a 2D study or three to a 3D study. While the p/n ratios are very variable (Table 1), datasets used in GM studies often have many more measurements than specimens. This is particularly common in, but not exclusive to,

1 anthropology, the discipline in which semilandmark methods for the analysis of curves and surfaces were
2 developed and are widely employed to study human evolution (Bookstein, 1997; Gunz and Mitteroecker, 2013;
3 Slice, 2005). Semilandmarks are typically closely spaced sets of arbitrary points used to ‘discretize’ anatomical
4 features, such as curves and surfaces, that are devoid of clearly corresponding landmark points; therefore, they
5 can greatly increase the number of variables in a study. Indeed, a propensity for morphometrics to employ large
6 numbers of variables has become especially evident in the last decade, thanks to new, cheaper and faster
7 instruments for the acquisition and analysis of 3D images. For instance, almost 60% of about 1000 entries,
8 retrieved at the end of 2018 in Publish or Perish (<https://harzing.com/resources/publish-or-perish>) using google
9 scholar to search “geometric morphometrics AND semilandmarks”, were papers published since 2013.

10

11 **Description of the bgPCA method**

12 An important topic in biology is the description and interpretation of group differences in multivariate spaces
13 Various approaches have been suggested to summarize among group variation in scatterplots (ordination
14 methods) and to classify individuals in groups. Yet, today’s most commonly multivariate technique for
15 separating groups is still multi-group linear discriminant analysis (DA), also known as canonical variates
16 analysis (CVA), originally proposed by Fisher (Fisher, 1936) and Mahalanobis (Mahalanobis, 1936). However, a
17 limit for using DA/CVA in a study is that, for statistical reliability, it requires sample sizes greatly exceeding the
18 count of variables in the analysis (Mitteroecker and Bookstein, 2011), and indeed it is not even computationally
19 defined if $p > n - g$. In these instances, a between-group PCA (bgPCA) has been suggested as an interesting
20 potential alternative to explore group structure. To our knowledge, this method was originally proposed by
21 Yendle and MacFie (1989) who called it “discriminant principal components analysis” (DPCA), though it does
22 not involve a standardization by the within-group variation as in DA and CVA. Another early paper is Culhane
23 et al. (2002), who applied it to the analysis of high-dimensional microarray data. While bgPCA has similarities
24 with discriminant functions, but also, as discussed by Boulesteix (2005), has relationships to partial least-squares
25 dimension reduction methods. Compared to DA/CVA, bgPCA is just a PCA and does not involve standardizing
26 the variables based on the variation within groups (Seetah et al. 2012). Also, as with DA/CVA, bgPCA has been
27 used for classification, and thus for predicting group affiliation based on bgPCs, an aim which should be
28 achieved with a cross-validation, as exemplified by leave-one-out jack-knife used in Culhane et al. (2002) and
29 Seetah et al. (2012). However, in contrast to a DA/CVA (Kovarovic et al. 2011; Mitteroecker and Bookstein,
30 2011), a bgPCA does not require $p \leq n - g$, which is why it has been claimed that “in ... between-group PCA
31 there is NO restriction on the number of variables” ([https://www.mail-](https://www.mail-archive.com/morphmet@morphometrics.org/msg05221.html)
32 [archive.com/morphmet@morphometrics.org/msg05221.html](https://www.mail-archive.com/morphmet@morphometrics.org/msg05221.html)).

33 The bgPCA procedure is used to reduce the dimensionality of multivariate data to just those dimensions
34 necessary to account for the differences among the g group means. Each sample is based on n_i individuals for a

1 total sample size of $n = \sum n_i$ or $n = gn_i$ in the case of equal sample sizes, as will be assumed here for
2 simplicity. A bgPCA is performed by projecting the original $n \times p$ data matrix, \mathbf{X} , onto the matrix, \mathbf{E} , of the
3 normalized eigenvector of the among-group SSCP matrix $\mathbf{A} = \sum_i^g n_i (\bar{\mathbf{x}}_i - \bar{\bar{\mathbf{x}}})' (\bar{\mathbf{x}}_i - \bar{\bar{\mathbf{x}}})$, where $\bar{\mathbf{x}}_i$ is the row
4 vector for the mean of the i th group and $\bar{\bar{\mathbf{x}}}$ is the grand mean vector. The \mathbf{A} matrix is at most of rank $g-1$ because
5 it is a PCA of just the matrix of g means so only the first $g-1$ eigenvalues can be greater than zero and thus only
6 the first $g-1$ columns of \mathbf{E} need to be retained. The $n \times (g-1)$ transformed data matrix is then $\mathbf{X}' = \mathbf{X}\mathbf{E}$. Based on
7 these, the transformed within-group and among-group SSCP matrices are $\mathbf{W}' = \mathbf{E}'\mathbf{W}\mathbf{E}$ and $\mathbf{A}' = \mathbf{E}'\mathbf{A}\mathbf{E} = \mathbf{\Lambda}$,
8 the diagonal matrix of the first $g-1$ eigenvalues of \mathbf{A} (note: the superscript “t” indicates matrix transpose; also,
9 while the equation for \mathbf{A} given above weights the mean for each group by its sample size, that may not be
10 appropriate for many applications, see Bookstein, 2019, but it is used here for generality). Importantly, the
11 number of bgPCs cannot be more than $g-1$. Thus, with just two groups, there are only two group means, and one
12 needs a single dimension to represent differences between two points; thus, when $g = 2$, there is only one bgPC.
13 If there are three groups, the differences among the three corresponding means can be fully described by a plane
14 passing through the three mean points, and thus by just two bgPCs. With $g > 3$ the rationale is the same and the
15 number of bgPCs is $g-1$, but the geometric representation is not as easy, because we cannot represent
16 multivariate spaces with more than three dimensions in a single scatterplot and even a 3D scatterplot (as with $g =$
17 4) can be difficult to interpret (Mitteroecker et al. 2005).

18

19 **Sampling experiments**

20 To investigate the effect of varying p/n ratios on bgPCA, sampling experiments were performed using both
21 isotropic data (independent variables with equal means and variances called Model 1 below) and data
22 constructed from an actual morphometric study but with no true differences among the group means (called
23 Models 2-3 below). Fig. 1 shows the result of bgPCAs using $g = 3$ groups with the same true means (i.e., no real
24 group differences), a constant total sample size ($n=120$), and an increasingly larger numbers of variables ($p=12$,
25 120 or 360). On the left (Fig. 1a) are bgPCA plots for isotropic data (Model 1, below) for $g = 3$ groups of
26 identical size ($n_i = n/3 = 40$). On the right (Fig. 1b), the same n_i , g and p are used as in Fig. 1A but based on
27 correlated morphometric variables from real data, which have been randomly divided into three groups so that
28 there are no real group differences. Convex hulls for each group are shown in order to identify group
29 memberships for each sample. Rather than showing the groups superimposed as one might expect, because there
30 are no true differences, Fig. 1 shows that bgPCA created an apparent clustering of the samples around their
31 group means as first noticed by one of us (AC). The groups appear increasingly distinct from one another as the
32 p/n ratio increases because larger numbers of variables are used. The effect is particularly evident for isotropic
33 data and less pronounced but still present for correlated variables.

1 The sampling experiments, shown in Fig. 1, were based on two different models, one (Fig. 1a) being the
2 same as model 1 (below) and the other (Fig. 1b) being similar to models 2-3 (below). In all instances, there are
3 no true differences among the means of the groups and the groups have the same size. Thus, in more detail, the
4 models used in the more extensive sampling experiments described below, were:

5 Model 1: A purely isotropic model with p independent random normally distributed variables, each with μ
6 $= 0$ and $\sigma = 1$. This model was used for Figs. 1a, 2, and 4 below.

7 Model 2&3: Random normally distributed variables with the same true covariance matrix as that of a real
8 morphometric dataset, but with all means equal to zero:

9 Model 2: Procrustes shape coordinates from a sample of 45 adult yellow-bellied marmot (*Marmota*
10 *flaviventris*) left hemimandibles. The original 2D configuration consists of 10 landmarks and 50
11 semilandmarks, with the semilandmarks slid in TPSRelw (Rohlf 2015) using the minimum
12 Procrustes distance criterion. This data matrix was then used to compute the covariance matrix
13 among the variables and its corresponding eigenvector matrix and eigenvalues. All eigenvectors
14 that had positive eigenvalues were retained. These were then used as described below to
15 generate random data matrices with the covariance matrix taken from the original dataset.

16 Model 3: Procrustes shape coordinates from a sample of 171 adult male vervet monkey skulls, which are
17 part of a larger published dataset (Cardini and Elton 2017). There were 86 3D skull landmarks
18 (Cardini et al. 2007; Cardini and Elton 2017). As with Model 2, as described below, these were
19 used to generate samples of random variables with the same true covariance matrix as in the
20 original data.

21
22 A sample, \mathbf{X} , from a population with a given true covariance matrix of Σ was generated using the
23 following relationship. $\mathbf{X} = \mathbf{Y}\mathbf{E}\mathbf{\Lambda}^{1/2}$, where \mathbf{Y} is an $n \times p$ matrix of independent random normally distributed
24 numbers with zero means and unit variances, \mathbf{E} is a matrix of the p , p -dimensional normalized eigenvectors of Σ ,
25 and $\mathbf{\Lambda}$ is the $p \times p$ diagonal matrix of its eigenvalues. A difference between sampling experiments using the
26 isotropic model (Model 1) and all others based on actual data (Models 2 and 3) is that the maximum number of
27 eigenvectors that can be computed is limited to the number of variables in the original study because the method
28 cannot construct more dimensions than are in the original data. For models 2 and 3, random samples of the rows
29 (corresponding to the variables) of matrix \mathbf{E} were used to generate variables. When the desired p was greater
30 than the original number of variables, variables were obtained by sampling the rows of \mathbf{E} with replacement.

31 In the sampling experiments that follow, the data were subjected to a bgPCA using code written by FJR
32 in MATLAB and group separation was assessed by computing an index of overlap between pairs of samples. Let

33 Q_{ij} be the proportion of individuals in a group i that are closer to the mean of group j . When the dispersions in
34 two groups i and j do not overlap, Q_{ij} will be equal to 0 and will approach 0.5 for a pair of groups that overlap

1 almost perfectly, because in that case a point is equally likely to be closest to either mean. The average, \bar{O}_{ij} for
2 all pairs of samples in a particular analysis is used as the measure of overlap. Initially, the amount of overlap
3 between convex hulls was considered, but this has some unsuitable properties (such as rapid decrease in the
4 probability of overlap as the number of dimensions increases even without the bgPCA transformation).

5

6 **What happens when n or g are changed relative to p ?**

7

8 Figure 2 summarizes the results of sampling experiments using \bar{O}_{ij} as a measure of overlap and varying g , n_i ,
9 and p . The figure uses n_i rather than n because the total size is not relevant for the computation of average
10 overlap as they depend on the relationships among pairs of samples and not the number of samples (and thus not
11 on the total sample size). The sampling experiments used $g = 3$ and 6 groups, sample sizes of $n_i = 20$ and 40 ,
12 and a range of values for the number of dimensions, p . Fig. 2 shows the expected outcome that overlap is larger
13 when p is smaller, n_i larger, and when there are more groups. The effect of p is strongest for the isotropic
14 model, but the effect is clear for all three models. The companion paper also demonstrates the effect of relaxing
15 the assumption of equal sample sizes.

16

17 **Mathematical interpretation: why the apparent separation of groups as p increases?**

18 Because the \bar{O}_{ij} index seems difficult to work with analytically, an alternative index inspired by the partitioning
19 of sums of squares in an anova or MANOVA was investigated for the simple null model (Model 1) used above,
20 i.e., samples of independent normally distributed random variables from the same population. As an
21 approximation, covariances among the variables are ignored (as they should be minimal for isotropic data) and
22 the group differences described in terms of the traces (sums of the diagonal elements) of the usual within and
23 among-groups sums of squares matrices, rather than the usual multivariate test statistics such as Wilks' Lambda
24 or Lawley-Hotelling U statistics, which require the computation of the matrix inversion and determinants of the
25 sums of squares matrices.

26 The reader should carefully note that all expressions in Table 2 are based just on the $g-1$ -dimensional
27 space of the bgPCA transformed data. Thus, the within-group sums of squares here only refers to that part of
28 total within group sums of squares expected in the $g-1$ -dimensional subspace. This table is *not* intended for and
29 should *never* be used for statistical testing (unlike that of a standard MANOVA, which would use the variation
30 in the p -dimensional space of the original variables even if resampling procedures are used), and is specifically
31 designed to produce an explanation for the apparent differences between groups such as shown Fig 1A.

1 As above, let \mathbf{A} represent the among-groups SSCP matrix based on all p variables and \mathbf{E} its matrix of
2 normalized eigenvectors. After projecting the data for all samples onto these vectors, one has a bgPCA
3 transformed data matrix $\mathbf{X}' = \mathbf{X}\mathbf{E}$. At most, only the first $g-1$ columns of \mathbf{E} and thus \mathbf{X}' are nonzero, so we will
4 use only the first $g-1$ columns. Let \mathbf{A}' be the among-groups SSCP matrix based on this transformed data matrix.
5 The sum of the eigenvalues of \mathbf{A} and \mathbf{A}' are equal because all of the variation among g means is captured in a $g-$
6 1-dimensional space. Similarly, one can define \mathbf{W} as the within-groups SSCP matrix using the original p
7 variables and \mathbf{W}' as the equivalent matrix using the projections of the data onto \mathbf{E} . Note that its trace $tr(\mathbf{W}')$
8 will, in general, be less than that of \mathbf{W} because only within-group variation in the $g-1$ dimensions in which the
9 means differ is preserved by the projection onto the $g-1$ -dimensional bgPCA space. The \mathbf{W} matrix has $n-g$
10 degrees of freedom and thus would require $\min(n-g, p)$ dimensions to account for all the within-group
11 variation.

12 Consider sampling experiments, such as described in the prior section for Model 1, where n_i specimens
13 are in each sample (assuming equal sample size, so that $n = gn_i$) are drawn from the same p -dimensional
14 multivariate normal distribution, that has a mean vector $\boldsymbol{\mu} = \mathbf{0}_p$ (a vector of p zeroes) and a covariance matrix
15 of $\boldsymbol{\Sigma} = \mathbf{I}_p$ (a $p \times p$ identity matrix). The true \mathbf{W} matrix would then be $(n-g)\mathbf{I}_p$ with $tr(\mathbf{W}) = p(n-g)$. The
16 true among groups variance component matrix, $\boldsymbol{\Sigma}_A$, is $\mathbf{0}_p$ because there are no true differences among the
17 population means. However, due to sampling error the expected among-groups covariance matrix is $\boldsymbol{\Sigma} + n_i \boldsymbol{\Sigma}_A$.
18 For the transformed data, the trace of the observed among-groups SSCP matrix is unchanged by the
19 transformation because all of the variation among g means will be accounted for by the $g-1$ eigenvectors.
20 However, the trace of the expected within-groups SSCP matrix will be reduced by the fraction $(g-1)/p$
21 assuming the remaining $n-g$ dimensions of within-group variation are just a random sample of the total variation
22 (reasonable here because, as mentioned above, there are no actual differences). These relations are conveniently
23 summarized in the format of a MANOVA table (Table 2), but just using the trace of each matrix divided by $g-1$
24 as a summary of the relative amounts of within and among samples variation captured in the bgPCA space only.

25 Note that the F_{iso} ratio defined in Table 2 (ratio of traces of among to within group MS using only the
26 $g-1$ bgPCs) is analogous to an F -ratio and is a function of just p and g . The subscript "iso" is to remind the
27 reader that it assumes isotropic data and is not the usual F employed for statistical testing (that, as mentioned,
28 should not be done using the equations of Table 2). Likewise, the "iso" in the subscript of R_{iso}^2 is to remind the
29 reader that this is not the usual squared multiple correlation coefficient, because this statistic, as it is
30 computed here using only the bgPCA variance, is only aimed at assessing the amount of group separation.

1 Thus, a value near zero would imply that groups account for little of the total variation and values near 1
2 imply that most of the variation is between groups rather than within groups. Figure 3 shows plots of
3 $R_{iso}^2 = p / (p + g(n_i - 1))$ as a function of n_i and p for $g = 3$ and 6 that illustrate how R_{iso}^2 increases as a
4 function of p (suggesting more distortion with more variables), but decreases as a function of n_i (indicating less
5 separation of groups with larger samples). For a given p and n_i , if g is smaller, and therefore also $n = gn_i$ is
6 smaller, the denominator in the R_{iso}^2 formula is reduced and R_{iso}^2 becomes larger, which is why the R_{iso}^2
7 surfaces in Figure 3 are higher for $g = 3$ than for $g = 6$. This is because adding more groups increases the
8 dimensionality of the bgPCA space and thus should account for a larger proportion of the within-group
9 variation.

10 The reader should note that larger R_{iso}^2 implies more separation and thus less overlap as measured by
11 \bar{O}_{ij} . Fig. 4 shows a scatterplot \bar{O}_{ij} as a function of R_{iso}^2 using the data from Fig. 2. The slope of the relationship
12 differs for data from the different models. The slope is less steep for the models with correlated variables. Within
13 each dataset the scatter corresponds to the effects of different values of g and n_i . The R_{iso}^2 statistic is somewhat
14 ad hoc, but Figure 4 (below) shows that it is a useful predictor of overlap for isotropic data.

15 The expressions in Table 2 are compared in Table 3 with the results from two sampling experiments.
16 The example in the upper half is for the case where there are fewer variables but larger sample sizes in each
17 group. The second for the case where the number of variables is larger and sample sizes are smaller. The values
18 are averages over 10,000 replications and show the close agreement with the expected values (given in
19 parentheses) computed using the formulas from Table 2.

20

21 **The effect of covariation among variables.**

22 The isotropic Model 1, used in the previous section, is based on the unrealistic assumption that the
23 variables are independent and have equal variances. Intuitively, one might expect that data with highly correlated
24 variables might be less prone to overestimating of the degree of group separation, and indeed the sampling
25 experiments presented in Figs. 1B, 2 and 4 do show less spurious separation for data with correlated variables
26 (i.e., the models using vervet and marmot covariance matrices). If, as an extreme case, because of a strong
27 correlation between variables, all of the variation in a dataset could be accounted for with just $g-1$ dimensions,
28 then all of the within-group variation would also be captured by the $g-1$ among-groups dimensions of the bgPCA
29 and no information would be lost. The R_{iso}^2 statistic described above should then be close to 0 and \bar{O}_{ij} should
30 measure the correct amount of overlap between groups, which should be close to 0.5 if there are no real groups).

31 In order to investigate the effect of covariation using sampling experiments, one must specify a model
32 for the pattern and strengths of the correlations. The selection of a model can be simplified because one can

1 rotate the data matrix to its principal axes, so that one need only consider models that differ in how the
2 eigenvalues decrease as a function of their number. For independent variables they would decrease somewhat
3 according to the Marchenko–Pastur formula (Bookstein 2017), but for highly correlated variables they would
4 decrease more rapidly. A very simple model is that the logs of the eigenvalues, $\ln(\lambda_i)$, decrease linearly as a
5 function of the log of their number, that is, $\ln(\lambda_i) = a - b \ln(i)$ or as $\lambda_i = e^{-bi}$, where a is a constant greater
6 than 0 (ignored here) and b determines how rapidly the eigenvalues decrease. This approach also models the
7 effect of unequal variances for the different variables. More realistic models with a factor structure could have
8 been investigated, but this model seems sufficient to illustrate the effect of different proportions of the variance
9 being accounted for by the first $g-1$ dimensions. Fig. 5A shows examples with b varied from 0 to 1. Larger
10 values of b yield increasingly rapid declines of successive eigenvalues, which imply stronger correlations among
11 variables.

12 Fig. 5B shows the results of, sampling experiments with $g = 3$ groups of $n_i = 20$ observations each, with
13 p ranging from 3 to 80, and each replicated 1000 times, for the b values used in Fig. 5A. The effect of increasing
14 correlations among the variables was to reduce the size of the expected R_{iso}^2 statistic implying a larger \bar{O}_{ij} and
15 thus less spurious clustering of points around the means. Many morphometric datasets follow patterns like that
16 shown for b equal to 1 or even larger values of b . For instance, the curve for the marmot mandible dataset
17 (Model 2) would be even more extreme than the curve shown for $b = 1$. The curve for the vervet data (Model 3)
18 is less extreme. Thus, it is not surprising that Fig. 1 shows that for data with highly correlated variables there
19 will be much less spurious group separation than that found for the isotropic model (Model 1).

20

21 Discussion

22 The primary focus of the present paper is on the reasons for the apparent clustering of points around the means
23 of arbitrary groups and predicting the magnitude of this distorted summary of group differences. In contrast, the
24 companion paper, Bookstein (2019), examines the effect of large p/n ratios on the bgPCA method in relationship
25 to the predictions of the Marchenko–Pastur theorem as described in Bookstein (2017), along with two other
26 aspects of the problem: the role of variations in sample sizes of the groups, and the effect of correlations among
27 the variables based on a variety of factor models. It also suggests ways of evaluating the impact of these effects
28 when analyzing actual data sets. We use sampling experiments and examples from our own field,
29 morphometrics, i.e. the quantitative study of biological forms (Blackith and Reyment 1971, Bookstein 1991).
30 However, the issue and its implications are general and apply similarly to multivariate data used to compare
31 groups in other fields such as genetics.

32 In our analyses we found that bgPCA ordinations may tend to exaggerate differences between groups
33 relative to the amount of within-group variation. In extreme cases, with few groups, small samples and very

1 many variables, bgPCA may consistently show perfect separation of the groups even when there are no true
2 differences among group means. This is in part because the $g-1$ dimensions of a bgPCA capture the entire
3 amount of variation among the g group means, but only a fraction of the variation within each group when $p > g-$
4 1. Thus, most of the variance within groups is lost, when p is much larger than $g-1$. With small samples, the
5 groups may appear quite distinct, but any apparent group differences will largely be an artefact of very large
6 sampling error (Cardini & Elton 2007; Cardini et al. 2015). This is because any inaccuracies in group mean
7 estimates are completely captured by the bgPCs, as if they were true differences, and used to define the $g-1-$
8 dimensional space.

9 Not surprisingly, one can also see in Figure 2 that, with the same p and g , larger samples overlap more
10 than smaller samples. Indeed, whether there are true differences or not, the range of variation within a sample is
11 expected to increase as its sample size increases and thus there is a greater chance of overlapping.

12 In summary, the distortion showing a consistent spurious degree of separation between groups is not a
13 promising property for a method that was proposed to analyze data with large numbers of variables and small
14 samples, but the picture is complex, because the gravity of the problem, as nicely exemplified by Figure 4, varies
15 sharply from case to case. Indeed, the severity of the distortion depends on both g and n_i relative to p , as well
16 as on how strongly variables covary and whether true differences are indeed present (a case which we did not
17 explore in our simulations). This is not unlike what Kovarovic et al. (2011) found in a study of discriminant
18 analysis (DA). They remarked that (p. 3012): “increasing the number of predictors may increase ... group
19 separation in scatterplots of non-cross-validated DFAs, even if those predictors are random numbers which do
20 not add any relevant information on group differences”. However, with bgPCA, this well-known problem of DA
21 may be even more serious, because in bgPCA there is no theoretical limit to the number of variables that can be
22 used to summarize groups and thus p can be much larger than n and g , as in many publications (Table 1).

23 Among the factors that might reduce the distortion, or even make it negligible, covariance is one of the
24 most interesting, as it is expected in most biological datasets. The reason why covariance mitigates against the
25 problem of bgPCA spurious group separation is that, with correlated variables, the number of independent
26 dimensions is effectively reduced and, therefore, operationally, it is as if the $p/g(n_i-1)$ ratio was smaller. The
27 degree to which it is smaller depends on the strength of the covariances. Yet, the problem is clearly still there, as
28 both separation and R_{iso}^2 still increase with p . Thus, the main conclusion is the same: even with covariances,
29 with a large $p/g(n_i-1)$ ratio, not only might one see groups that appear overly separated, as in our sampling
30 experiments, but also, if there are true groups, the differences will be inflated by a case-specific degree, which is
31 difficult to predict a priori.

32 There are many reasons to expect strong covariances in studies using Procrustes-based GM. Some
33 covariance is introduced by the fact that, for 2D data, the superimposition reduces the $2q$ -dimensional variation
34 of the raw coordinates (with q being the number of landmarks) to the $2q-4$ dimensions of shape space (Rohlf and

1 Slice, 1990). In addition, covariation will depend on factors such as the number and distribution of the
2 anatomical points. For example, landmarks that are very close together and closely spaced semilandmarks are
3 expected to be highly correlated (Cardini 2018). Thus, the marmot data includes slid semilandmarks and 90% of
4 the total variance in these data can be accounted for by just the first 10 PCs (out of the 44 possible because $n =$
5 45 and $p = 120$). By contrast, the vervet data requires 56 PCs (out of the 170 possible because $n = 171$ and $p =$
6 251) to account for the same percentage of total variance. Fig. 2 shows that the curves for the marmot data are
7 higher (more overlap and thus less false clustering) than the curves for the vervet data (less overlap and thus
8 stronger false separation of the groups). Note that these results do not suggest that one should purposely add
9 highly correlated variables to reduce the distortion expected in the results of a bgPCA. Adding perfectly
10 correlated variables to an existing dataset will not change the effective dimensionality of a dataset and thus will
11 not alter the degree of false clustering expected in the results of a bgPCA.

12

13 On the other hand, in datasets where strong correlations among variables are expected, such as is
14 common in GM, where additional covariance is introduced by the Procrustes superimposition itself (Rohlf and
15 Slice, 1990) and many semilandmarks are used (because physically close semilandmarks tend to covary
16 strongly), one might hope to circumvent some of the issues raised in this paper by reducing the number of
17 variables used in the bgPCA. Indeed, in GM studies, it is often the case that distance matrices among specimens
18 assessed using a few landmarks are highly correlated with those derived from the full set of landmarks plus
19 many semilandmarks (Skinner et al, 2009; Ferretti et al. 2013; Watanabe, 2018; Galimberti et al. 2019). This can
20 be assessed formally, for instance, through matrix correlations where testing whether full (all landmarks and
21 semilandmarks) and reduced (a subset of the full configuration) data matrices are highly correlated. Thus,
22 smaller ratios of $p/g(n_i - 1)$ can be achieved at the outset, simply by limiting the number of variables used in
23 the study. If this is done, the resulting visualizations of shape differences among specimens will be less detailed,
24 because fewer landmarks are used, but results of bgPCA will be less likely to be misleading.

25 It is important to bear in mind that scatterplots are not the only tool for assessing group differences.
26 Results from a bgPCA should be complemented by tests of significance, as well as by cross-validated
27 classifications of groups (e.g., Seetah et al. 2012). However, they must be performed using the full p -
28 dimensional space (unlike the statistics in the ‘*ad-hoc*’ MANOVA Tables 2-3, using only bgPCs with the
29 specific aim of assessing the magnitude of spurious group differences in the bgPCA sub-space). Wwith small
30 samples, and/or negligible group separation *in the full data space*, group differences using all p variables will be
31 non-significant, thus alerting the user that any appearance of group separation in bgPCA scatterplots should be
32 regarded with extreme suspicion. Also, as one of the main aims in the formulation of bgPCA by Culhane et al.
33 2002 was classification, the results should be checked by cross-validating bgPCAs in the full data space. Finding
34 a cross-validated accuracy only negligibly different from that expected by chance should warn users about likely
35 distortions in the scatterplots.

1
2
3
4
5
6
7
8
9
10
11
12
13
14
15
16
17
18
19
20
21
22
23
24
25
26
27
28
29
30
31
32
33
34

In conclusion, big datasets are increasingly common, but having very many variables does not ‘counterbalance’ the effect of small n ; it could make it worse, as shown here and in Bookstein (2019). Thus, we show that in attempting to assess group distinctiveness using bgPCA there is a potential trap, in that spurious apparent groupings may emerge in scatterplots, especially when the subspace spanned by the $g-1$ bgPCs does not adequately reflect within group variation, as is increasingly likely to happen when p/n is large and g is small. The appearance of spurious groups in bgPCA offers a good reminder of how a large number of descriptors might bring problems as well as benefits, with the problems sometimes potentially outweighing the benefits. Indeed, as with other methods (Hair et al. 2009; Bookstein, 2017), bgPCA provides another example of the potential perils of high dimensional data, and of the possible misuse of techniques and misinterpretation of findings, when the basic issues of sampling error and data dimensionality are not clearly borne in mind.

Acknowledgement:

We are very grateful to Jessica Grisenti, who carefully collected the marmot data for her undergraduate thesis and gave AC permission to use them. The authors appreciate the most helpful comments of Julien Claude who reviewed this paper.

Dedications:

The paper is dedicated to the memories of Nicola Saino (1961 - 2019) and Dennis Slice (1958 - 2019).

Nicola was one of the greatest Italian ethologists, Professor of Animal Behaviour at the University of Milan, and extraordinary ornithologist: AC will always remember with fondness the day Nicola introduced him, and other biology students, to the wonders of birdwatching; he will also never forget his brilliant example as a teacher and researcher; and he will greatly miss the passionate fights, with him, over methods.

Dennis Slice Professor in the Dept. of Scientific Computing, The Florida State University was an Evolutionary biologist and Ecologist who made major contributions to morphometrics through his scientific and software contributions, by maintaining and moderating the MORPHMET discussion group and by being a tireless supporter and educator of students and colleagues. For his contributions, he was awarded the Rohlf Medal for Excellence in Morphometric Methods and Applications in 2017. Not only was he a tireless advocate of his field but he was a wonderful colleague, always available and always thoughtful. We will miss him greatly as both a scientist and a colleague.

Compliance with Ethical Standards

Conflict of interest. The authors declare that they have no conflicts of interest.

References

- 1 Astúa, D. (2009). Evolution of Scapula Size and Shape in Didelphid Marsupials (didelphimorphia: Didelphidae).
2 *Evolution*, 63(9), 2438-2456, doi:10.1111/j.1558-5646.2009.00720.x.
- 3 Baab, K. L. (2016). The role of neurocranial shape in defining the boundaries of an expanded Homo erectus
4 hypodigm. *Journal of Human Evolution*, 92, 1-21, doi:10.1016/j.jhevol.2015.11.004.
- 5 Benazzi, S., Douka, K., Fornai, C., Bauer, C. C., Kullmer, O., Svoboda, J., et al. (2011). Early dispersal of
6 modern humans in Europe and implications for Neanderthal behaviour. *Nature*, 479(7374), 525-528,
7 doi:10.1038/nature10617.
- 8 Blackith, R. E. and R. A. Reyment (1971). *Multivariate Morphometrics*. New York, Academic Press.
- 9 Bookstein, F. L. (1991). *Morphometric tools for landmark data: Geometry and Biology*. New York, Cambridge
10 Univ. Press.
- 11 Bookstein, F. L. (1997). Landmark methods for forms without landmarks: morphometrics of group differences
12 in outline shape. *Medical Image Analysis*, 1, 225–243.
- 13 Bookstein, F. L. (2017). A Newly Noticed Formula Enforces Fundamental Limits on Geometric Morphometric
14 Analyses. *Evolutionary Biology*, 44(4), 522–541. doi:10.1007/s11692-017-9424-9
- 15 Bookstein, F. L. (2018). *A Course in Morphometrics for Biologists*. Cambridge Univ. Press.
- 16 Bookstein, F. L. (2019). Pathologies of Between-Groups Principal Components Analysis in Geometric
17 Morphometrics. *Evolutionary Biology*, submitted.
- 18 Bookstein, F., Schäfer, K., Prossinger, H., Seidler, H., Fieder, M., Stringer, C., et al. (1999). Comparing frontal
19 cranial profiles in archaic and modern Homo by morphometric analysis. *The Anatomical Record*, 257(6),
20 217-224, doi:10.1002/(SICI)1097-0185(19991215)257:6<217::AID-AR7>3.0.CO;2-W.
- 21 Boulesteix, A.-L., 2005. A note on between-group PCA. *Int. J. Pure Appl. Math.*, 19, 359-366.
- 22 Cardini, A. (2003). The Geometry of the Marmot (Rodentia: Sciuridae) Mandible: Phylogeny and Patterns of
23 Morphological Evolution. *Systematic Biology*, 52(2), 186-205, doi:10.1080/10635150390192807.
- 24 Cardini, A. (2018). Integration and Modularity in Procrustes Shape Data: Is There a Risk of Spurious Results?
25 *Evolutionary Biology*. doi:10.1007/s11692-018-9463-x
- 26 Cardini, A., & Elton, S. (2007). Sample size and sampling error in geometric morphometric studies of size and
27 shape. *Zoomorphology*, 126(2), 121–134. doi:10.1007/s00435-007-0036-2
- 28 Cardini, A., & Elton, S. (2008). Does the skull carry a phylogenetic signal? Evolution and modularity in the
29 guenons. *Biological Journal of the Linnean Society*, 93(4), 813-834, doi:10.1111/j.1095-
30 8312.2008.01011.x.
- 31 Cardini, A., Jansson, A., & Elton, S. (2007). A geometric morphometric approach to the study of

- 1 ecogeographical and clinal variation in vervet monkeys. *Journal of Biogeography*, 34(10), 1663–1678.
2 doi:10.1111/j.1365-2699.2007.01731.x
- 3 Cardini, A., & Elton, S. (2017). Is there a "Wainer's rule"? Testing which sex varies most as an example analysis
4 using GueSDat, the free Guenon Skull Database. *Hystrix, the Italian journal of mammalogy*, 28(2), 147–
5 156. doi.org/10.4404/hystrix-28.2-12139
- 6 Cardini, A., & O'Higgins, P. (2004). Patterns of morphological evolution in Marmota (Rodentia, Sciuridae):
7 geometric morphometrics of the cranium in the context of marmot phylogeny, ecology and conservation.
8 *Biological Journal of the Linnean Society*, 82(3), 385-407, doi:10.1111/j.1095-8312.2004.00367.x.
- 9 Cardini, A., & Loy, A. (2013). On growth and form in the "computer era": from geometric to biological
10 morphometrics. *Hystrix, the Italian journal of mammalogy*, 24, 1-5. doi.org/10.4404/hystrix-24.1-8749
- 11 Cardini, A., Seetah, K., & Barker, G. (2015). How many specimens do I need? Sampling error in geometric
12 morphometrics: testing the sensitivity of means and variances in simple randomized selection
13 experiments. *Zoomorphology*, 134(2), 149–163. doi:10.1007/s00435-015-0253-z
- 14 Chemisquy, M. A., Prevosti, F. J., Martin, G., & Flores, D. A. (2015). Evolution of molar shape in didelphid
15 marsupials (Marsupialia: Didelphidae): analysis of the influence of ecological factors and phylogenetic
16 legacy. *Zoological Journal of the Linnean Society*, 173(1), 217-235, doi:10.1111/zoj.12205.
- 17 Chiozzi, G., Bardelli, G., Ricci, M., De Marchi, G., & Cardini, A. (2014). Just another island dwarf? Phenotypic
18 distinctiveness in the poorly known Soemmerring's Gazelle, *Nanger soemmerringii* (Cetartiodactyla:
19 Bovidae), of Dahlak Kebir Island. *Biological Journal of the Linnean Society*, 111(3), 603-620,
20 doi:10.1111/bij.12239.
- 21 Cooke, S. B., & Terhune, C. E. (2015). Form, Function, and Geometric Morphometrics. *The Anatomical Record*,
22 298(1), 5-28, doi:10.1002/ar.23065.
- 23 Corti, M., Aguilera, M., & Capanna, E. (2001). Size and shape changes in the skull accompanying speciation of
24 South American spiny rats (Rodentia: Proechimys spp.). *Journal of Zoology*, 253(4), 537-547,
25 doi:10.1017/S0952836901000498.
- 26 Cucchi, T., Hulme-Beaman, A., Yuan, J., & Dobney, K. (2011). Early Neolithic pig domestication at Jiahu,
27 Henan Province, China: clues from molar shape analyses using geometric morphometric approaches.
28 *Journal of Archaeological Science*, 38(1), 11-22, doi:10.1016/j.jas.2010.07.024.
- 29 Culhane, A. C., Perrière, G., Considine, E. C., Cotter, T. G., & Higgins, D. G. (2002). Between-group analysis
30 of microarray data. *Bioinformatics*, 18(12), 1600–1608. doi:10.1093/bioinformatics/18.12.1600
- 31 Dapporto, L., Petrocelli, I., & Turillazzi, S. (2011). Incipient morphological castes in *Polistes gallicus* (Vespidae,
32 Hymenoptera). *Zoomorphology*, 130(3), 197-201, doi:10.1007/s00435-011-0130-3.

- 1 Domjanic, J., Seidler, H., & Mitteroecker, P. (2015). A combined morphometric analysis of foot form and its
2 association with sex, stature, and body mass. *American Journal of Physical Anthropology*, 157(4), 582-
3 591, doi:10.1002/ajpa.22752.
- 4 Ferretti, A., Cardini, A., Crampton, J. S., Serpagli, E., Sheets, H. D., & Štorch, P. (2013). Rings without a lord?
5 Enigmatic fossils from the lower Palaeozoic of Bohemia and the Carnic Alps. *Lethaia*, 46(2), 211-222.
6 doi.org/10.1111/let.12004
- 7 Fisher, R. A. (1936). The use of multiple measurements in taxonomic problems. *Annals of eugenics*, 7(2), 179-
8 188. doi.org/10.1111/j.1469-1809.1936.tb02137.x
- 9 Franchini, P., Fruciano, C., Spreitzer, M. L., Jones, J. C., Elmer, K. R., Henning, F., et al. (2014). Genomic
10 architecture of ecologically divergent body shape in a pair of sympatric crater lake cichlid fishes.
11 *Molecular Ecology*, 23(7), 1828-1845, doi:10.1111/mec.12590.
- 12 Franklin, D., Cardini, A., Flavel, A., & Kuliukas, A. (2013). Estimation of sex from cranial measurements in a
13 Western Australian population. *Forensic Science International*, 229(1), 158.e151-158.e158,
14 doi:10.1016/j.forsciint.2013.03.005.
- 15 Fruciano, C., Celik, M. A., Butler, K., Dooley, T., Weisbecker, V., & Phillips, M. J. (2017). Sharing is caring?
16 Measurement error and the issues arising from combining 3D morphometric datasets. *Ecology and*
17 *Evolution*, 7(17), 7034-7046, doi:10.1002/ece3.3256.
- 18 Fruciano, C., Franchini, P., Raffini, F., Fan, S., & Meyer, A. (2016). Are sympatrically speciating Midas cichlid
19 fish special? Patterns of morphological and genetic variation in the closely related species *Archocentrus*
20 *centrarchus*. *Ecology and Evolution*, 6(12), 4102-4114, doi:10.1002/ece3.2184.
- 21 Fruciano, C., Tigano, C., & Ferrito, V. (2011). Geographical and morphological variation within and between
22 colour phases in *Coris julis* (L. 1758), a protogynous marine fish. *Biological Journal of the Linnean*
23 *Society*, 104(1), 148-162, doi:10.1111/j.1095-8312.2011.01700.x.
- 24 Galimberti, F., S. Sanvito, M. C. Vinesi and A. Cardini (2019). Nose-metrics of wild southern elephant seal
25 (*Mirounga leonina*) males using photogrammetry and geometric morphometry. *Journal of Zoological*
26 *Systematics & Evolutionary Research*, DOI: 10.1111/jzs.12276.
- 27 Gómez-Robles, A., Olejniczak, A. J., Martín-Torres, M., Prado-Simón, L., & Castro, J. M. B. d. (2011).
28 Evolutionary Novelties and Losses in Geometric Morphometrics: A Practical Approach Through
29 Hominin Molar Morphology. *Evolution*, 65(6), 1772-1790, doi:10.1111/j.1558-5646.2011.01244.x.
- 30 Gonzalez, P. N., Kristensen, E., Morck, D. W., Boyd, S., & Hallgrímsson, B. (2013). Effects of growth hormone
31 on the ontogenetic allometry of craniofacial bones. *Evolution & Development*, 15(2), 133-145,
32 doi:10.1111/ede.12025.

- 1 Green, D. J., Sugiura, Y., Seitelman, B. C., & Gunz, P. (2015). Reconciling the convergence of supraspinous
2 fossa shape among hominoids in light of locomotor differences. *American Journal of Physical*
3 *Anthropology*, 156(4), 498-510, doi:10.1002/ajpa.22695.
- 4 Gunz, P., Ramsier, M., Kuhrig, M., Hublin, J.-J., & Spoor, F. (2012). The mammalian bony labyrinth
5 reconsidered, introducing a comprehensive geometric morphometric approach. *Journal of Anatomy*,
6 220(6), 529-543, doi:10.1111/j.1469-7580.2012.01493.x.
- 7 Gunz, P., & Mitteroecker, P. (2013). Semilandmarks: a method for quantifying curves and surfaces. *Hystrix, the*
8 *Italian journal of mammalogy*, 24 (1) 103–109. doi.org/10.4404/hystrix-24.1-6292
- 9 Hair, J.F., Black, W.C., Babin, B.J. and Anderson, R.E., 2009. *Multivariate Data Analysis, 7th Edition*. Pearson
10 Prentice Hall.
- 11 Houle, D. (2009). Colloquium Paper: Numbering the hairs on our heads: The shared challenge and promise of
12 phenomics, *Proceedings of the National Academy of Sciences (USA)*, 107 (suppl. 1), 1793–1799.
13 doi.org/10.1073/pnas.0906195106
- 14 Hublin, J.-J., Ben-Ncer, A., Bailey, S. E., Freidline, S. E., Neubauer, S., Skinner, M. M., et al. (2017). New
15 fossils from Jebel Irhoud, Morocco and the pan-African origin of Homo sapiens. *Nature*, 546(7657),
16 289-292, doi:10.1038/nature22336.
- 17 Ivanović, A., Sotiropoulos, K., Džukić, G., & Kalezić, M. L. (2009). Skull size and shape variation versus
18 molecular phylogeny: a case study of alpine newts (*Mesotriton alpestris*, Salamandridae) from the
19 Balkan Peninsula. *Zoomorphology*, 128(2), 157-167, doi:10.1007/s00435-009-0085-9.
- 20 Izenman, A. J. (2008) *Modern Statistical Techniques: Regression, Classification, and Manifold Learning*.
21 Springer.
- 22 Klenovšek, T., & Jojić, V. (2016). Modularity and cranial integration across ontogenetic stages in Martino's
23 vole, *Dinaromys bogdanovi*. *Contributions to Zoology*, 85(3), 275-289, doi:10.1163/18759866-
24 08503002.
- 25 Knigge, R. P., Tocheri, M. W., Orr, C. M., & McNulty, K. P. (2015). Three-Dimensional Geometric
26 Morphometric Analysis of Talar Morphology in Extant Gorilla Taxa from Highland and Lowland
27 Habitats. *The Anatomical Record*, 298(1), 277-290, doi:10.1002/ar.23069.
- 28 Kovarovic, K., Aiello, L. C., Cardini, A., & Lockwood, C. A. (2011). Discriminant function analyses in
29 archaeology: are classification rates too good to be true? *Journal of Archaeological Science*, 38(11),
30 3006–3018.
- 31 Kubiak, B. B., Gutiérrez, E. E., Galiano, D., Maestri, R., & Freitas, T. R. O. d. (2017). Can Niche Modeling and
32 Geometric Morphometrics Document Competitive Exclusion in a Pair of Subterranean Rodents (Genus

- 1 Ctenomys) with Tiny Parapatric Distributions? *Scientific Reports*, 7(1), 1-13, doi:10.1038/s41598-017-
2 16243-2.
- 3 Mahalanobis, P. C. (1936). On the generalized distance in statistics. *Proceedings National Institute of Science*,
4 India, 2(1), 49-55.
- 5 Mitteroecker, P., & Bookstein, F. (2011). Linear Discrimination, Ordination, and the Visualization of Selection
6 Gradients in Modern Morphometrics. *Evolutionary Biology*, 38(1), 100–114. doi:10.1007/s11692-011-
7 9109-8
- 8 Mitteroecker, P., Gunz, P., & Bookstein, F. L. (2005). Heterochrony and geometric morphometrics: a
9 comparison of cranial growth in *Pan paniscus* versus *Pan troglodytes*. *Evolution & Development*, 7(3),
10 244–258. doi:10.1111/j.1525-142X.2005.05027.x
- 11 Neubauer, S., Gunz, P., Leakey, L., Leakey, M., Hublin, J.-J., & Spoor, F. (2018). Reconstruction, endocranial
12 form and taxonomic affinity of the early Homo calvaria KNM-ER 42700. *Journal of Human Evolution*,
13 121, 25-39, doi:10.1016/j.jhevol.2018.04.005.
- 14 Oxnard, C., & O'Higgins, P. (2011). Biology Clearly Needs Morphometrics. Does Morphometrics Need
15 Biology? *Biological Theory*, 4(1), 84–97. doi:i: 10.1162/biot.2009.4.1.84
- 16 Pallares, L. F., Turner, L. M., & Tautz, D. (2016). Craniofacial shape transition across the house mouse hybrid
17 zone: implications for the genetic architecture and evolution of between-species differences.
18 *Development Genes and Evolution*, 226(3), 173-186, doi:10.1007/s00427-016-0550-7.
- 19 Reyment, R. A. (2010). Morphometrics: An Historical Essay. In A. M. T. Elewa (Ed.), *Morphometrics for*
20 *Nonmorphometricians* (Vol. 124, 9–24). Berlin, Heidelberg: Springer Berlin Heidelberg.
21 <http://www.springerlink.com/content/c6743496220p4892/>. Accessed 21 December 2011.
- 22 Ritzman, T. B., Terhune, C. E., Gunz, P., & Robinson, C. A. (2016). Mandibular ramus shape of
23 *Australopithecus sediba* suggests a single variable species. *Journal of Human Evolution*, 100, 54-64,
24 doi:10.1016/j.jhevol.2016.09.002.
- 25 Rohlf, F. J., & Slice, D. (1990). Extensions of the Procrustes Method for the Optimal Superimposition of
26 Landmarks. *Systematic Zoology*, 39(1), 40–59. doi:10.2307/2992207
- 27 Sanfilippo, P. G., Cardini, A., Sigal, I. A., Ruddle, J. B., Chua, B. E., Hewitt, A. W., et al. (2010). A geometric
28 morphometric assessment of the optic cup in glaucoma. *Experimental Eye Research*, 91(3), 405-414,
29 doi:10.1016/j.exer.2010.06.014.
- 30 Sansalone, G., Colangelo, P., Kotsakis, T., Loy, A., Castiglia, R., Bannikova, A. A., et al. (2018). Influence of
31 Evolutionary Allometry on Rates of Morphological Evolution and Disparity in strictly Subterranean
32 Moles (Talpinae, Talpidae, Lipotyphla, Mammalia). *Journal of Mammalian Evolution*, 25(1), 1-14,

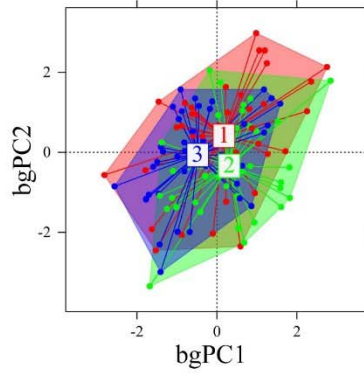
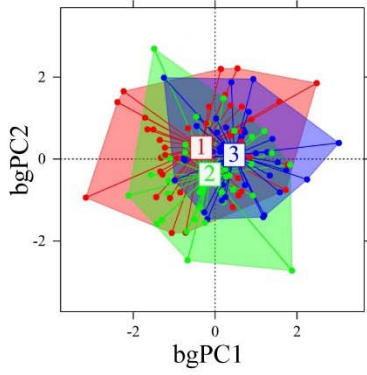
- 1 doi:10.1007/s10914-016-9370-9.
- 2 Schlager, S. (2017). Morpho and Rvcg – Shape Analysis in R. In G. Zheng, S. Li, & G. Szekely (Eds.),
3 *Statistical Shape and Deformation Analysis*, (pp. 217–256). Academic Press.
- 4 Schlager, S., & Rüdell, A. (2015). Analysis of the human osseous nasal shape—population differences and
5 sexual dimorphism. *American Journal of Physical Anthropology*, 157(4), 571-581,
6 doi:10.1002/ajpa.22749.
- 7 Seetah, T. K., Cardini, A., & Miracle, P. T. (2012). Can morphospace shed light on cave bear spatial-temporal
8 variation? Population dynamics of *Ursus spelaeus* from Romualdova pećina and Vindija, (Croatia),
9 *Journal of Archaeological Science*, 39(2), 500–510. doi.org/10.1016/j.jas.2011.10.005
- 10 Serb, J. M., Sherratt, E., Alejandrino, A., & Adams, D. C. (2017). Phylogenetic convergence and multiple shell
11 shape optima for gliding scallops (Bivalvia: Pectinidae). *Journal of Evolutionary Biology*, 30(9), 1736-
12 1747, doi:10.1111/jeb.13137.
- 13 Siberchicot, A., Julien-Laferrrière, A., Dufour, A.-B., Thioulouse, J., & Dray, S. (2017). adegraphics: An S4
14 Lattice-Based Package for the Representation of Multivariate Data. *The R Journal*, 9(2), 198–212.
15 doi.org/10.32614/RJ-2017-042.
- 16 Skinner, M. M., Gunz, P., Wood, B. A., & Hublin, J. J. (2009). How many landmarks? Assessing the
17 classification accuracy of Pan lower molars using a geometric morphometric analysis of the occlusal
18 basin as seen at the enamel-dentine junction. In *Comparative Dental Morphology* (Vol. 13, pp. 23-29).
19 Karger Publishers. DOI: 10.1159/000242385
- 20 Slice, D. E. (2005). Modern morphometrics. In *Modern morphometrics in physical anthropology* (pp. 1-45).
21 Springer, Boston, MA.
- 22 Souto-Lima, R. B., & Millien, V. (2014). The influence of environmental factors on the morphology of red-
23 backed voles *Myodes gapperi* (Rodentia, Arvicolinae) in Québec and western Labrador. *Biological*
24 *Journal of the Linnean Society*, 112(1), 204-218, doi:10.1111/bij.12263.
- 25 Torres□Tamayo, N., García□Martínez, D., Zloliniski, S. L., Torres□Sánchez, I., García□Río, F., & Bastir, M.
26 (2018). 3D analysis of sexual dimorphism in size, shape and breathing kinematics of human lungs.
27 *Journal of Anatomy*, 232(2), 227-237, doi:10.1111/joa.12743.
- 28 Watanabe A (2018) How many landmarks are enough to characterize shape and size variation? *PLoS ONE*,
29 13(6): e0198341. <https://doi.org/10.1371/journal.pone.0198341>
- 30 Yendle, P. W., & MacFie, H. J. (1989). Discriminant principal components analysis. *Journal of chemometrics*,
31 3(4), 589-600. doi.org/10.1002/cem.1180030407

1 Figures and Tables with captions

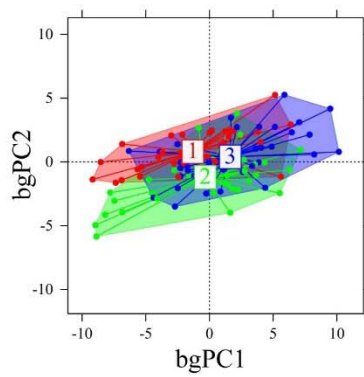
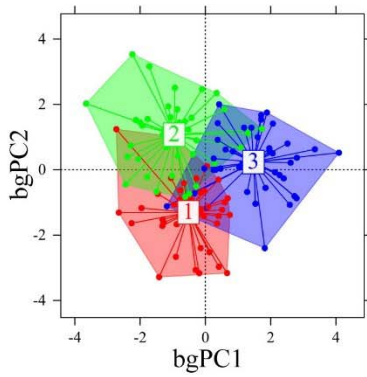
2

$n=120$

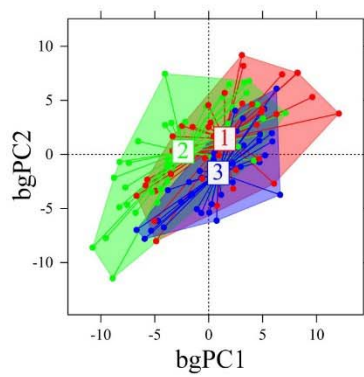
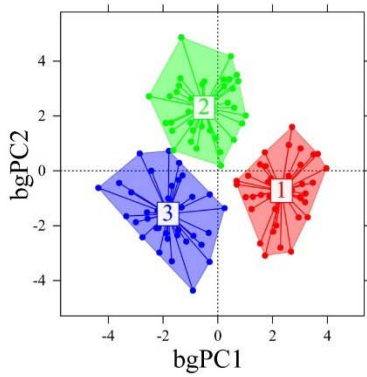
$p=12$



$p=120$



$p=360$



multivariate normal
isotropic

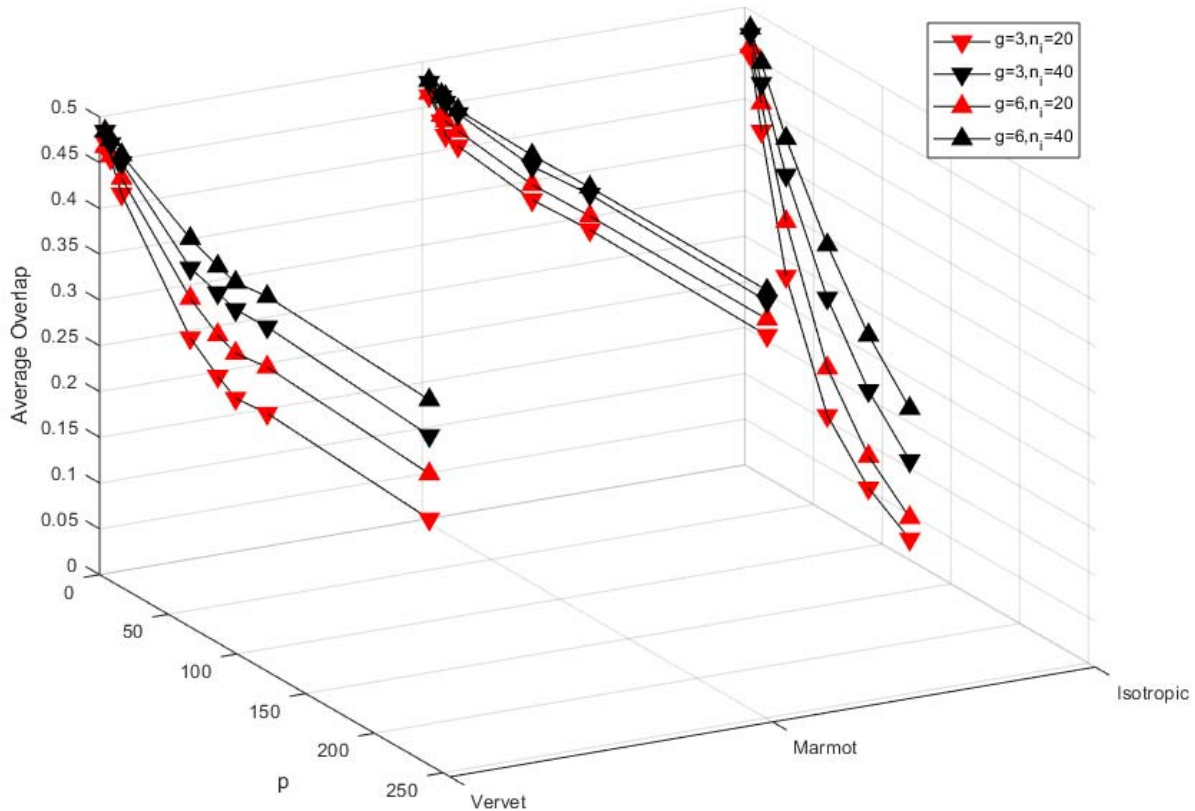
cranial linear
measures

(a)

(b)

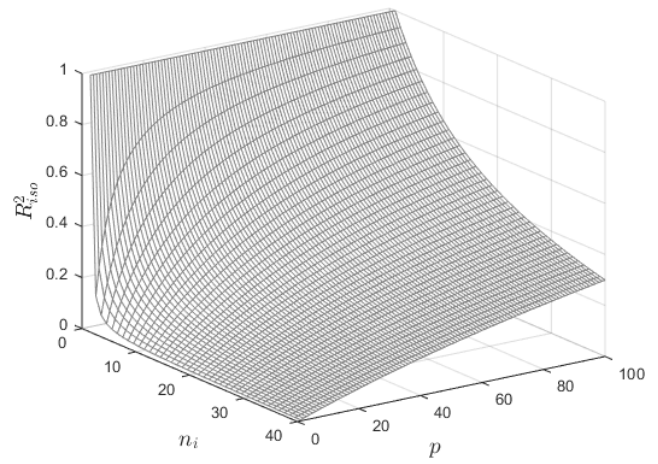
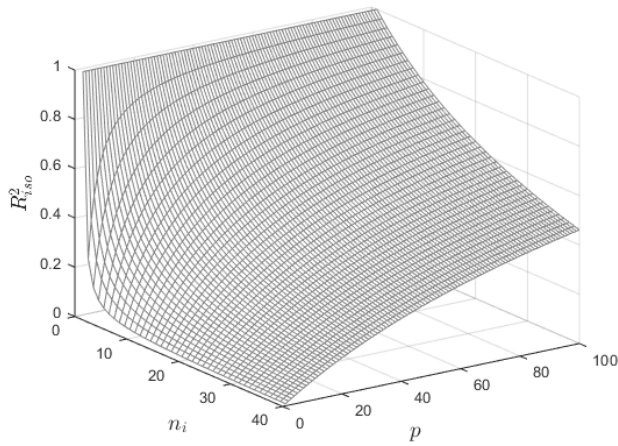
3

1 Fig. 1. bgPCA scatterplots (computed using Morpho – Schlager, 2017 – and drawn using Adegraphics
 2 – Siberchicot et al. 2017) showing the increasing spurious separation of random groups as p/n
 3 increases: (a) normal multivariate isotropic (i.e., uncorrelated variables) model; (b) normal multivariate
 4 model with covarying variables (based on the covariance matrix of a set of adult male vervet cranial
 5 linear measurements).
 6



7
 8 Fig. 2. Plots of \bar{O}_{ij} (average overlap between groups) from sampling experiments for three models:
 9 Mod1 (isotropic), Mod2 (Marmot Procrustes shape coordinates), and Mod3 (Vervet Procrustes shape
 10 coordinates), using $g = 3$ or 6 groups and $n_i = 20$ and 40 . In all models, there is less overlap when there
 11 are fewer groups and smaller n_i as p increases.

1
2

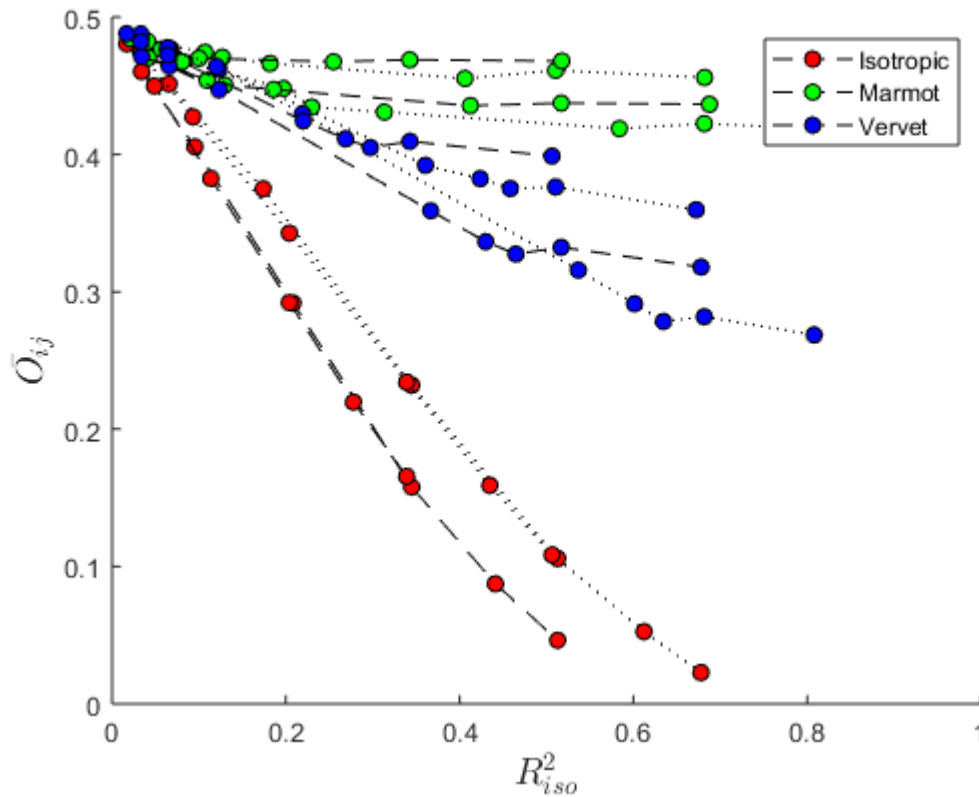


3

4 Fig. 3. Expected relationship between R^2_{iso} and n_i and p . A. For $g = 3$. B. For $g = 6$ groups. Note that
5 the height of the surface is lower when larger sample sizes are larger, more groups, and fewer variables
6 (see Table 2).

7

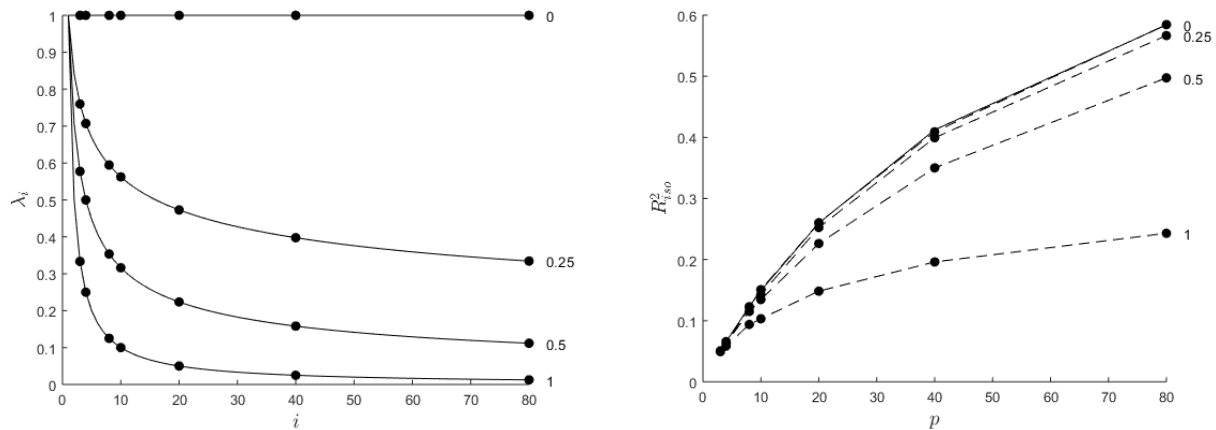
8



2

3 Fig. 4. A scatterplot of \bar{O}_{ij} (average overlap between groups) against R_{iso}^2 using the results of the
 4 sampling experiment shown in Fig. 2. Within each dataset it shows a tight negative relationship
 5 between \bar{O}_{ij} and R_{iso}^2 with a shallower slope for datasets that have more highly correlated variables.
 6 Dotted lines connect points for $g = 3$ groups and dashed lines for $g = 6$ groups. For isotropic data R_{iso}^2
 7 is smaller when there are more groups. Curves for different sample sizes are plotted but
 8 indistinguishable.

1
2



3
4

5 Fig. 5. A. Plot showing the effect of varying b the rate of decrease of the eigenvalues (λ) for a
6 hypothetical covariance matrix with $p = 80$ variables. The curve for $b = 1$ is similar to those usually

7 observed in morphometric data. B. Plot showing R^2_{iso} values for the results of sampling experiments
8 for simulated data based on the models shown in Fig 5A. The slope b was varied from 0 to 1 to
9 increase the level of correlation among the variables. Experiments were performed using 1000

10 replicates for $g = 3$ groups of size $n_i = 20$. The solid line shows the expected relationship,

11 $R^2_{iso} = p / (p + g(n_i - 1))$, for uncorrelated data that closely matches the results from this sampling

12 experiment. This plot shows that for the bgPCA method the proportion of the total variance accounted
13 for by the variance among groups is expected to increase as the number of variables increases but less

14 so as the overall level of correlation among the variables increases. For large n_i , the slope of the curve
15 would approach the abscissa if the correlations were such that only the first $g-1$ eigenvalues were

16 greater than 0.

17
18
19

1 Tables and captions

2

3 Table 1. Examples of papers showing the wide range of p/N and N/g ratios used in Procrustean GM
 4 studies involving groups. The number of shape coordinates is used as a proxy for p (i.e., without
 5 considering the loss of dimensions in the superimposition and, if applicable, because of sliding
 6 semilandmarks or 'symmetrization'). N is either the number of individuals or, if individuals were
 7 averaged in the between group analyses, the number of taxa. The average number of specimens per
 8 group (with g being the number of groups) is also shown. Studies using bgPCA are emphasized in bold
 9 while the columns with p/N and N/g ratios are emphasized in light grey.

10

study	semilandmarks?	N	p	p/N	g	p/g	t
Hublin et al., 2017 (root surface)	yes	69	1650	23.9	5	330	
Neubauer et al., 2018	yes	127	2805	22.1	5	561	
Torres-Tamayo et al., 2017	yes	80	1245	15.6	4	311	
Knigge et al., 2015	yes	87	567	6.5	4	142	
Gunz et al., 2012	yes	80	312	3.9	2	156	
Bookstein et al., 1999	yes	21	50	2.4	8	6	
Schlager & Ruedel, 2015	yes	534	1110	2.1	4	278	
Baab, 2016 (Bodo dataset)	-	24	42	1.8	2	21	
Gonzalez et al., 2013	-	59	93	1.6	5	19	
Sansalone et al., 2018	-	53	72	1.4	2	36	
Domjanic et al., 2015	yes	134	170	1.3	2	85	
Benazzi et al., 2011	yes	38	48	1.3	3	16	
Green et al., 2015	yes	279	258	0.9	5	52	
Gomez-Robles et al., 2011	yes	129	94	0.7	10	9	
Fruciano et al., 2016 (fish body)	yes	61	44	0.7	2	22	
Chiozzi et al., 2018 (fish body)	yes	62	44	0.7	5	9	
Kubiak et al., 2017	-	85	60	0.7	4	15	
Cucchi et al., 2011	yes	114	80	0.7	9	9	
Fruciano et al., 2017 (all landmarks)	-	138	93	0.7	23	4	
Serb et al., 2017	yes	933	606	0.6	6	101	
Pallares et al., 2016	-	249	132	0.5	9	15	
Chemisquy et al., 2014 (upper molar)	yes	103	52	0.5	5	10	
Sanfilippo et al., 2010	-	160	72	0.5	2	36	
Seetah et al., 2012	-	67	24	0.4	4	6	
Cooke & Terhune, 2015	-	169	60	0.4	7	9	
Ritzman et al., 2016	yes	315	90	0.3	4	23	
Klenovšek et al., 2016	-	215	58	0.3	6	10	
Franklin et al., 2013	-	400	93	0.2	2	47	
Cardini & Elton, 2008	-	1126	258	0.2	30	9	
Fruciano et al., 2011	-	223	40	0.2	9	4	
Corti et al., 2001	-	277	44	0.2	12	4	
Ivanovic et al., 2009	-	166	26	0.2	9	3	
Dapporto et al., 2011	-	130	20	0.2	2	10	

	Cardini & O'Higgins, 2004	-	354	52	0.1	14	4
	Souto-Lima & Millien (skull)	-	212	30	0.1	3	10
	Franchini et al., 2014	-	297	40	0.1	3	13
	Cardini, 2003	-	388	18	0.0	14	1
1	Astua, 2008	-	1079	38	0.0	56	1

2 Table 2. MANOVA-style table summarizing expectations after a bgPCA transformation with g equal-
3 sized samples of size n_i all drawn from the same p -dimensional normally distributed population with
4 mean $\boldsymbol{\mu}=\mathbf{0}_p$ (a vector of p zeros) and covariance matrix $\boldsymbol{\Sigma}=\mathbf{I}_p$ (a $p \times p$ identity matrix). Because the
5 table assumes equal-sized samples, $n=gn_i$. The expressions for the traces of the SS matrices are given
6 along with their MS after division by degrees of freedom. The F_{iso} ratio is also given in analogy to the
7 usual F ratio and the proportion of the total variation accounted for by differences among means, R_{iso}^2 ,
8 is also given. Note that these are not the usual F and R^2 coefficients from an anova or a multiple
9 regression analysis – they are expected values assuming the isotropic model, unlike a standard
10 MANOVA where one estimates between-group variance relative to within-group using *all* original
11 variables, here computations are only within the $g-1$ dimensions of the bgPCA transformed data and
12 cannot be used for statistical testing. This means that the within-group component shown in the table
13 only refers to the residual variance left unexplained by groups in the $g-1$ dimensional bgPCA space
14 (i.e., the within-group variation one sees in the scatterplots such as in Fig. 1).

15

Source of variation	df	Trace SS	Trace MS	F_{iso} Ratio
Among	$g-1$	$tr(\mathbf{A}') = p(g-1)$	p	$p/(g-1)$
Within	$g(n_i-1)$	$tr(\mathbf{W}') = \frac{(g-1)}{p} pg(n_i-1) = (g-1)g(n_i-1)$	$g-1$	
Total	$g(n_i-1)$	$tr(\mathbf{A}' + \mathbf{W}') = (g-1)p + (g-1)g(n_i-1)$ $= (g-1)(p + g(n_i-1))$	$(p + g(n_i-1))/(gn_i-1)$	

R_{iso}^2	$\frac{p(g-1)}{(g-1)(p+g(n_i-1))} = \frac{p}{p+g(n_i-1)}$
-------------	---

1
2

3

1
 2 Table 3. Two examples of sampling experiments showing averages based on 10,000 replicates of the
 3 null model with all samples drawn from the same independent and normally distributed population
 4 with mean 0 and variance 1. Expected values based on Table 2 are given in parentheses. The upper
 5 table is an example with smaller p and large sample sizes. The lower table has a larger p and smaller
 6 sample sizes. As with Table 2, all computations are done using only using the $g-1 = 2$ dimensions from
 7 a bgPCA. Note that, unlike the formulas in Table 1, the traces are divided by $g-1$ to give an average
 8 diagonal element.
 9

$p = 20, g = 3, n_i = 40$				
Source of variation	df	Trace SS/($g-1$)	Trace MS/($g-1$)	F_{iso} Ratio
Among	2	20.0380 (20)	10.0190 (10)	10.1124 (10)
Within	117	116.9471 (117)	0.9995 (1)	
Total	59	136.9851 (137)	1.1511 (1.1513)	
$R_{iso}^2 = 0.1460$ (0.1460)				

10

$p = 80, g = 3, n_i = 10$				
Source of variation	df	Trace SS/($g-1$)	Trace MS/($g-1$)	F_{iso} Ratio
Among	2	79.96975 (80)	39.9849 (40)	41.4724 (40)
Within	27	27.0319 (27)	1.0012 (1)	
Total	29	107.0016 (107)	3.6897 (3.6897)	
$R_{iso}^2 = 0.7469$ (0.7477)				

11
 12
 13